Design, Synthesis and Evaluation of Novel Benzimidazoles, Benzothiazoles and Benzofurans Incorporating Pyrazole Moiety as Antiangiogenic Agents

Authors
S. M. Rida[1], A. M. Youssef[1], M. H. Badr[1], A. Malki[2], Z. A. Sherif[3], A. S. Sultan[2,3]

Affiliations
[1] Department of Pharmaceutical Chemistry, Faculty of Pharmacy, Alexandria University, Alexandria, Egypt
[2] Department of Biochemistry, Faculty of Science, Alexandria University, Alexandria, Egypt
[3] Department of Oncology, Georgetown University Medical Center, Washington DC, USA

Key words
- Benzimidazole
- benzothiazole
- benzofuran and pyrazole derivatives
- human umbilical vein endothelial cell (HUVEC)
- vascular endothelial growth factor receptor (VEGF-2)
- Antiangiogenic activity
- Antiproliferative effect

received 12.08.2011
accepted 07.11.2011

Bibliography
DOI http://dx.doi.org/10.1055/s-0031-1295483
Arzneimittelforschung 2012; 62: 63–74

ISSN 0004-4172

Correspondence
Amal M. Youssef
Associate Prof
Department of Pharmaceutical Chemistry
Faculty of Pharmacy
Alexandria University
1 Elkhartoum square-Azarita
21521 Alexandria
Egypt
Tel.: +2/(03)/4871 317
Fax: +2/(03)/4873 273
ayoussef65@yahoo.com

Ahmed S. Sultan
Associate Prof
Department of Biochemistry
Faculty of Science
Alexandria University
Alexandria
Egypt
dr_asultan@WHO.net

Abstract

Novel benzimidazoles, benzothiazoles and benzofurans incorporating pyrazole moiety have been synthesized and screened for their antiangogenic activities, by testing their ability to inhibit human umbilical vein endothelial cell (HUVEC) proliferation, cord formation and migration in response to chemoattractant. 3 compounds **19**, **23** and **26** showed antiangiogenic activities at non-cytotoxic concentrations. Compound **19** was the most active with chemotaxis activity data nearly comparable to that of the positive control, TNP-470. Compound **42** showed a significant cytotoxic effect on the tested cancer cell lines and less antiangiogenesis activity compared to compounds **19**, **23** and **26**. All the tested compounds, in contrary to TNP-470, interfered with the migratory function of HUVECs in response to vascular endothelial growth factor rather than the endothelial cells proliferation or cord formation. Moreover, a docked pose of compounds **19** and **26** was obtained bound to kinase insert domain receptor using Molecular Operating Environment module.

Introduction

Angiogenesis, the formation of new capillaries from existing vasculature, is a normal physiological event that occurs during embryonic growth, wound healing and the menstrual cycle. Abnormal regulation of angiogenesis has been found to be involved in the pathogenesis of several disorders including diabetic retinopathy [1], inflammation [2], rheumatoid arthritis [3], psoriasis [4], age-related macular degeneration [5], and cancer [6,7].

It has been well recognized that angiogenesis is essential for solid tumor growth and metastasis [8,9]. Tumors that lack an adequate vasculature become necrotic or apoptotic and do not grow beyond a limited size. Thus, new means to retard angiogenesis have shown promise as potential cancer therapies. Antiangiogenic therapy, which targets activated endothelial cells, presents several advantages over therapy directed against tumor cells; it targets genetically stable, normal endothelial cells that should not develop resistance [10,11].

Angiogenesis is regulated by the expression of a variety of growth factors including vascular endothelial growth factor (VEGF), other growth factors and cytokines [12,13]. Until recently, investigations in this area have focused on VEGF and its receptor tyrosin kinase VEGFR-2 (or KDR, kinase insert domain receptor) [14,15]. Thus inhibition of the VEGF signaling pathway has emerged as one of the most valuable new approaches in the treatment of cancers as approximately 60% of malignant tumors express high concentrations of VEGF [16]. VEGF is perhaps the most specific for endothelial cells. When VEGF binds to its receptor it triggers signaling pathways that result in endothelial cell migration, differentiation and proliferation, increased vascular permeability and release of endothelial cell precursors from the bone marrow, VEGF also prevents endothelial cell apoptosis [17].

Strategies to inhibit the VEGF pathway include antibodies directed against VEGF or VEGFR, soluble VEGFR/VEGFR hybrids, soluble analogues of the VEGFR (VEGF-Trap) and tyrosine kinase inhibitors. One of the earliest strategies to inhibit VEGF activity involved the use of antibodies directed against VEGFRs. For example, preclinical data with anti-VEGFR-2 antibodies demonstrated decreased VEGF-induced signaling, decreased angiogenesis and decreased primary and metastatic growth in a variety of tumor systems [18].

On the other hand, the importance of COX-2 in carcinogenesis and brain tumor progression is highlighted by the detection of COX-2 in brain tumor and COX-2 overexpression in gliomas associated with poor prognosis. Targeting COX-2 with selective COX inhibitors as celecoxib has proven effective to reduce human glioblastoma cell viability in vivo [19]. Celecoxib is the only drug approved by FDA for adjuvant treatment of patients with familial adenomatous polyposis [20]. Several mechanisms have been proposed in various tumor models, celecoxib activates apoptotic protein P53 leading to antiproliferative effect and tumor angiogenesis [21].

According to a scientific report, a novel 1,3,4- trisubstituted pyrazole derivative **a** (◉ **Fig. 1**) were found to exhibit significant antiangiogenic profile at non-cytotoxic doses and was superior to celecoxib [22].

Careful literature survey revealed that a 2-aminobenzimidazole derivative **b** (◉ **Fig. 1**) was identified as potent inhibitor of VEGFR-2. The modeling study proved that the benzimidazole core is oriented in the hydrophobic pocket neighboring the ATP binding site [23].

In a recent approach, some novel benzimidazole urea derivatives **c** (◉ **Fig. 1**) were discovered as potent inhibitors of TIE-2 (tyrosine kinase containing Ig and EGF homology domains) and VEGFR-2 which are implicated in angiogenesis [24].

Moreover, novel benzimidazole derivatives **d** (◉ **Fig. 1**) with unique antiangiogenic characteristics have been reported where they inhibited VEGF [25].

Furthermore, a 2-arylimidazo[2,1-b][1,3]benzothiazole derivative **e** (◉ **Fig. 1**) was reported as a selective growth inhibitor of endothelial cells [26].

In view of the above mentioned findings, the aim of the present study is to synthesize and investigate the in vitro antiangiogenic activity of some novel benzimidazoles and their bioisosteres. The target compounds incorporate in their molecules the pharmacophores that are believed to be responsible for the biological significance of some relevant chemotherapeutic agents such as the trisubstituted pyrazole functionality as in angiogenic COX-2 inhibitor; celecoxib. The substitution pattern of the pyrazole ring was carefully selected so as to confer different electronic environments to the molecules. So we report herein the synthesis and the in vitro antiangiogenic activity of some novel structure hybrids incorporating both the benzimidazole moiety or its bioiostere with the pyrazole ring through different linkages. In the first scheme, the benzimidazole or benzothiazole scaffold is linked with substituted pyrazole through a vinyl 2 carbon bridge or through azavinyl linker, while in the second scheme the benzofuran ring is directly attached to the pyrazole moiety through a single bond. This combination was suggested in an attempt to investigate the influence of such hybridization and structure variation on the anticipated biological activity hoping to obtain synergestic chemotherapeutic activity with higher selectivity and less toxicity.

Materials and Methods

Chemistry

Melting points were determined in open glass capillaries on a Gallenkamp melting point apparatus and were uncorrected. The infrared (IR) spectra were recorded on Perkin-Elmer 1430 infrared spectrophotometer using the KBr plate technique. ^{1}H-NMR spectra were determined on Jeol spectrometer (500 MHz) at the Microanalytical unit, Faculty of Science, Alexandria University and on a Varian spectrometer (300 MHz), Faculty of Science, Cairo University using tetramethylsilane (TMS) as the internal standard and DMSO-d_6 as the solvent (Chemical shifts in δ,

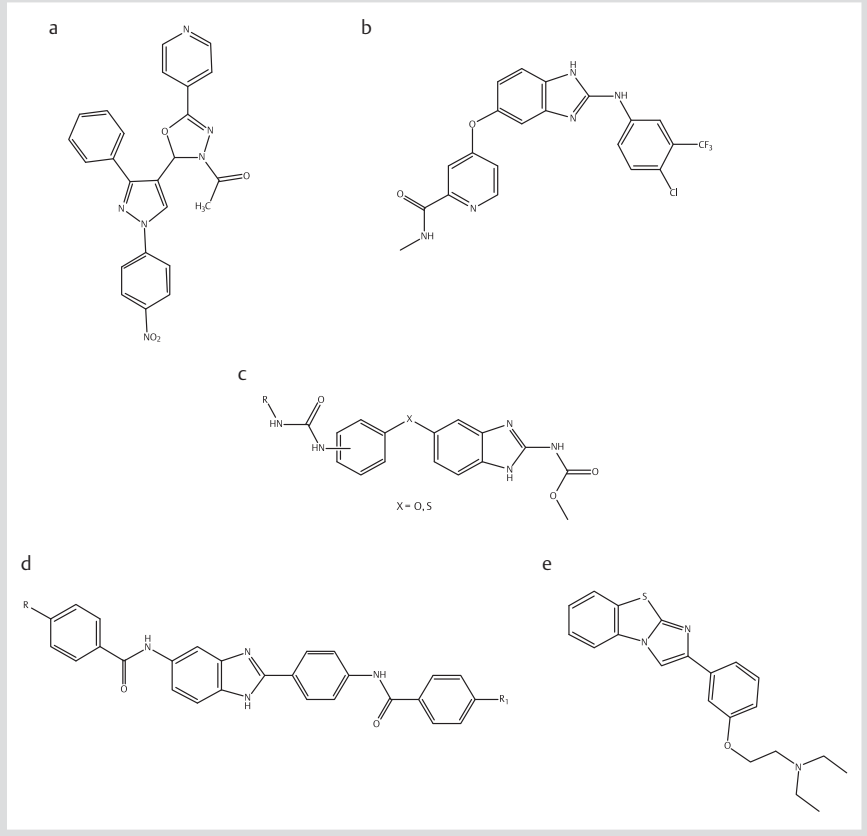

Fig. 1 Structure of lead compounds **a–e**.

ppm). Splitting patterns were designated as follows: s: singlet; d: doublet; m: multiplet. MS were run on a Finnigan mass spectrometer model SSQ/7000 (70 eV, Thermo Electron Corporation). Microanalyses were performed at the Microanalytical Unit, Faculty of Science, Cairo University, Egypt and the found values were within ± 0.4% of the theoretical values. Follow-up of the reactions and checking the homogeneity of the compounds were made by TLC on silica gel-protected glass plates and the spots were detected by exposure to UV-lamp at λ 254.

3-(4-Methylphenyl)-1-(4-nitrophenyl)-1*H*-pyrazole-4-carbaldehyde (14)

To an ice-cold dimethylformamide (25 g, 30 ml, 0.34 mole), $POCl_3$ (10 g, 6 ml, 0.066° mole) was added dropwise with stirring over a period of 30 min. Stirring was continued for further 1 h keeping the reaction temperature at 0 °C. Compound **6** [27] (8.1 g, 0.03 mole) was then added and the reaction mixture was heated at 60–70 °C with stirring for 4 h, allowed to cool and poured onto ice-water mixture. The obtained mixture was boiled and the obtained precipitate was filtered, washed with water, dried and crystallized from dioxane. Yield: 76%, mp: 181–183 °C. IR (cm^{-1}): 1700 (C=O); 1632 (C=N). ^{1}H-NMR (δ ppm): 1.54 (s, 1H, CH_3); 7.57 (d, *J* = 8.4 Hz, 2 H, *p*-tolyl-$C_{3,5}$-H); 7.83 (d, *J* = 8.4 Hz, 2H, *p*-tolyl-$C_{2,6}$-H); 8.24 (d, *J* = 9.2 Hz, 2H, *p*-nitrophenyl-$C_{2,6}$-H); 8.39 (d, *J* = 9.2 Hz, 2H, *p*-nitrophenyl-$C_{3,5}$-H); 9.23 (s, 1H, pyrazole-C_5-H); 9.62 (s, 1H, CHO). Anal. Calcd for $C_{17}H_{13}N_3O_3$ (307.31): C, 66.44; H, 4.26; N, 13.67. Found: C, 66.76; H, 4.31; N, 13.45.

2-(1*H*-Benzimidazol-2-yl)-3-(1,3-diaryl-1*H*-pyrazol-4-yl) acrylonitrile (17–28)

To a stirred solution of benzazol-2-ylacetonitrile (0.002 mole) in absolute ethanol (10 ml), triethylamine (0.2 ml) and the appropriate pyrazole aldehyde **9–16** (0.002 mole) were added. The reaction mixture was heated under reflux for 1–3 h during which yellow crystals separated out. The crystalline product was filtered, washed with water, dried and crystallized from the proper solvent.

2-(1H-Benzimidazol-2-yl)-3-(1,3-diphenyl-1H-pyrazol-4-yl)acrylonitrile (17). Yield: 72%, mp: > 300 °C (EtOH). IR (cm^{-1}): 3300 (NH); 2247 (C≡N); 1609 (C=N). ^{1}H-NMR (δ ppm): 7.18–7.21 (m, 2 H, benzimidazole-$C_{5,6}$-H); 7.45–7.71 (m, 10 H, benzimidazole-$C_{4,7}$-H and phenyl-H); 7.77 (d, *J* = 7.2 Hz, 2 H, phenyl-$C_{2,6}$-H); 7.99 (s, 1H, =CH); 9.29 (s, 1H, pyrazole-C_5-H); 12.80 (s, 1H, NH, D_2O exchangeable). MS, m/z (rel. Abund. %): 388 (18.5) M^{+}+1; 387 (77.8) M^{+}; 386 (47.7); 311 (25.9); 310 (100); 283 (11.1); 282 (7.6); 281 (8.8); 180 (7.1); 77 (23.9); 51 (16.0). Anal. Calcd for $C_{25}H_{17}N_5$ (387.44): C, 77.50; H, 4.42; N, 18.08. Found: C, 77.27; H, 4.15; N, 17.89.

2-(1H-Benzimidazol-2-yl)-3-(1-phenyl-3-p-tolyl-1H-pyrazol-4-yl) acrylonitrile (18). Yield: 86%, mp: > 300 °C (EtOH). IR (cm^{-1}): 3254(NH); 2231 (C≡N); 1627 (C=N). ^{1}H-NMR (δ ppm): 2.36 (s, 1H, CH_3); 7.20–7.23 (m, 2H, benzimidazole-$C_{5,6}$-H); 7.39 (d, *J* = 7.4 Hz, 2H, *p*-tolyl-$C_{3,5}$-H); 7.55–7.62 (m, 9H, benzimidazole-$C_{4,7}$-H, phenyl-H and *p*-tolyl-$C_{2,6}$-H); 8.12 (s, 1H, =CH); 9.31 (s, 1H, pyrazole-C_5-H); 12.91 (s, 1H, NH, D_2O exchangeable). Anal. Calcd for $C_{26}H_{19}N_5$ (401.46): C, 77.79; H, 4.77; N, 17.44. Found: C, 77.52; H, 4.98; N, 17.08.

2-(1H-Benzoimidazol-2-yl)-3-(3-(4-chlorophenyl)-1-phenyl-1H-pyrazol-4-yl)acrylonitrile (19). Yield: 63%, mp: > 300 °C (Dioxane/EtOH). IR (cm^{-1}): 3229 (NH); 2226 (C≡N); 1630 (C=N). ^{1}H-NMR (δ ppm): 7.19–7.22 (m, 2H, benzimidazole-$C_{5,6}$-H); 7.41–7.63 (m, 7H, benzimidazole-$C_{4,7}$-H and phenyl-H); 7.72 (d, *J* = 8.4 Hz, 2H, *p*-chlorophenyl-$C_{2,6}$-H); 7.91 (d, *J* = 8.4 Hz, 2H, *p*-chlorophenyl-$C_{3,5}$-H); 8.09 (s, 1H, =CH); 9.19 (s, 1H, pyrazole-C_5-H); 13.10 (s, 1H, NH, D_2O exchangeable). Anal. Calcd for $C_{25}H_{16}ClN_5$ (421.88): C, 71.17; H, 3.82; N, 16.60. Found: C, 70.88; H, 3.62; N, 16.56.

2-(1H-Benzimidazol-2-yl)-3-(3-(4-bromophenyl)-1-phenyl-1H-pyrazol-4-yl)acrylonitrile (20). Yield: 69%, mp: > 300 °C (dioxane). IR (cm^{-1}): 3264 (NH); 2243 (C≡N); 1618 (C=N). ^{1}H-NMR (δ ppm): 7.21–7.24 (m, 2H, benzimidazole-$C_{5,6}$-H); 7.50–7.65 (m, 7H, benzimidazole-$C_{4,7}$-H and phenyl- H); 7.74 (d, *J* = 8.4 Hz, 2H, *p*-bromophenyl-$C_{2,6}$-H); 7.95 (d, *J* = 8.4 Hz, 2H, *p*-bromophenyl-$C_{3,5}$-H); 8.13 (s, 1H, =CH); 9.21 (s, 1H, pyrazole-C_5-H); 12.88 (s, 1H, NH, D_2O exchangeable). Anal. Calcd for $C_{25}H_{16}BrN_5$ (466.33): C, 64.39; H, 3.46; N, 15.02. Found: C, 64.45; H, 3.67; N, 14.77.

2-(1H-Benzimidazol-2-yl)-3-(1-(4-nitrophenyl)-3-phenyl-1H-pyrazol-4-yl)acrylonitrile (21). Yield: 75%, mp: > 300 °C (dioxane/EtOH). IR (cm^{-1}): 3240 (NH); 2229 (C≡N); 1626 (C=N). ^{1}H-NMR (δ ppm): 7.22–7.25 (m, 2H, benzimidazole-$C_{5,6}$-H); 7.49–7.62 (m, 5H, benzimidazole-$C_{4,7}$-H and phenyl-$C_{3,4,5}$-H); 7.71 (d, *J* = 7.65 Hz, 2H, phenyl-$C_{2,6}$-H); 8.14 (s, 1H, =CH); 8.21 (d, *J* = 9.2 Hz, 2H, *p*-nitrophenyl-$C_{2,6}$-H); 8.43 (d, *J* = 9.2 Hz, 2H, *p*-nitrophenyl-$C_{3,5}$-H); 9.30 (s, 1H, pyrazole-C_5-H); 13.02 (s, 1H, NH, D_2O exchangeable). Anal. Calcd for $C_{25}H_{16}N_6O_2$ (432.43): C, 69.44; H, 3.73; N, 19.43. Found: C, 69.72; H, 3.54; N, 19.67.

2-(1H-Benzimidazol-2-yl)-3-(1-(4-nitrophenyl)-3-p-tolyl-1H-pyrazol-4-yl)acrylonitrile (22). Yield: 65%, mp: > 300 °C (dioxane/EtOH). IR (cm^{-1}): 3250 (NH); 2251 (C≡N); 1626 (C=N). ^{1}H-NMR (δ ppm): 2.43 (s, 1H, CH_3); 7.23–7.26 (m, 2H, benzimidazole-$C_{5,6}$-H); 7.41 (d, *J* = 7.8 Hz, 2H, *p*-tolyl-$C_{3,5}$-H); 7.62–7.65 (m, 4H, benzimidazole-$C_{5,6}$-H and *p*-tolyl-$C_{2,6}$-H); 8.14 (s, 1H, =CH); 8.24 (d, *J* = 9.2 Hz, 2H, *p*-nitrophenyl-$C_{2,6}$-H); 8.45 (d, *J* = 9.2 Hz, 2H, *p*-nitrophenyl-$C_{3,5}$-H); 9.40 (s, 1H, pyrazole-C_5-H). Anal. Calcd for $C_{26}H_{18}N_6O_2$ (446.46): C, 69.95; H, 4.06; N, 18.82. Found: C, 70.14; H, 4.09; N, 18.53.

2-(1H-Benzimidazol-2-yl)-3-(3-(4-chlorophenyl)-1-(4-nitrophenyl)-1H-pyrazol-4-yl)acrylonitrile (23). Yield: 73%, mp: > 300 °C (dioxane). IR (cm^{-1}): 3259 (NH); 2233 (C≡N); 1619 (C=N). ^{1}H-NMR (δ ppm): 7.22–7.25 (m, 2H, benzimidazole-$C_{5,6}$-H); 7.49–7.52 (m, 2H, benzimidazole-$C_{4,7}$-H); 7.62 (d, *J* = 8.4 Hz, 2H, *p*-chlorophenyl-$C_{2,6}$-H); 7.89 (d, *J* = 8.4 Hz, 2H, *p*-chlorophenyl-$C_{3,5}$-H); 8.11 (s, 1H, =CH); 8.22 (d, *J* = 9.2 Hz, 2H, *p*-nitrophenyl-$C_{2,6}$-H); 8.44 (d, *J* = 9.2 Hz, 2H, *p*-nitrophenyl-$C_{3,5}$-H); 9.36 (s, 1H, pyrazole-C_5-H); 12.99 (s, 1H, NH, D_2O exchangeable). Anal. Calcd for $C_{25}H_{15}ClN_6O_2$ (466.88): C, 64.31; H, 3.24; N, 18.00. Found: C, 64.63; H, 3.45; N, 18.21.

2-(1H-Benzimidazol-2-yl)-3-(3-(4-bromophenyl)-1-(4-nitrophenyl)-1H-pyrazol-4-yl)acrylonitrile (24). Yield: 74%, mp: > 300 °C (DMF/H_2O). IR (cm^{-1}): 3247 (NH); 2227 (C≡N); 1609 (C=N). ^{1}H-NMR (δ ppm): 7.24–7.27 (m, 2H, benzimidazole-$C_{5,6}$-H); 7.50–7.53 (m, 2H, benzimidazole-$C_{4,7}$-H); 7.66 (d, *J* = 8.4 Hz, 2H, *p*-bromophenyl-$C_{2,6}$-H); 7.91 (d, *J* = 8.4 Hz, 2H, *p*-bromophenyl-$C_{3,5}$-H); 8.13 (s, 1H, =CH); 8.24 (d, *J* = 9.2 Hz, 2H, *p*-nitrophenyl-$C_{2,6}$-H); 8.46 (d, *J* = 9.2 Hz, 2H, *p*-nitrophenyl-$C_{3,5}$-H);

9.29 (s, 1H, pyrazole-C_5-H); 12.75 (s, 1H, NH, D_2O exchangeable). Anal. Calcd for $C_{25}H_{15}BrN_6O_2$ (511.33): C, 58.72; H, 2.96; N, 16.44. Found: C, 59.01; H, 2.79; N, 16.57.

2-(Benzothiazol-2-yl)-3-(1,3-diphenyl-1H-pyrazol-4-yl)acrylonitrile (25). yield: 87%, mp: 170–172 °C (dioxane/EtOH). IR (cm^{-1}): 2237 (C≡N); 1608 (C=N); 1298, 1026 (C-S-C). ^{1}H-NMR (δ ppm): 7.21–7.24 (m, 3H, phenyl-$C_{3,4,5}$-H); 7.43–7.61 (m, 9H, benzothiazole-H and phenyl-H); 7.78 (d, *J* = 7.2 Hz, 2H, phenyl-$C_{2,6}$-H); 8.45 (s, 1H, =CH); 9.31 (s, 1H, pyrazole-C_5-H). Anal. Calcd for $C_{25}H_{16}N_4S$ (404.49): C, 74.23; H, 3.99; N, 13.85; S 7.93. Found: C, 74.50; H, 4.04; N, 13.56; S 8.22.

2-(Benzothiazol-2-yl)-3-(1-phenyl-3-p-tolyl-1H-pyrazol-4-yl) acrylonitrile (26). Yield: 78%, mp: 196–198 °C (dioxane/EtOH). IR (cm^{-1}): 2242 (C≡N); 1630 (C=N); 1255, 1085 (C-S-C). ^{1}H-NMR (δ ppm): 2.33 (s, 1H, CH_3); 7.35 (d, *J* = 7.4 Hz, 2H, *p*-tolyl-$C_{3,5}$-H); 7.53–7.72 (m, 11H, benzothiazole-H, phenyl-H and *p*-tolyl-$C_{2,6}$-H); 8.39 (s, 1H, =CH); 9.28 (s, 1H, pyrazole-C_5-H). MS, m/z (rel. Abund. %): 371 (3.9); 370 (20.4); 369 (35.5); 368 (100); 367 (44.1); 366 (60.5); 352 (8.6); 148 (12.5); 136 (16.4); 118 (15.1); 116 (13.8); 109 (11.8); 90 (16.4); 78 (28.9); 77 (96.7); 76 (14.5); 69 (13.8); 65 (48.7); 51 (64.5). Anal. Calcd for $C_{26}H_{18}N_4S$ (418.51): C, 74.62; H, 4.34; N, 13.39; S 7.66. Found: C, 74.99; H, 4.25; N, 13.71; S 7.81.

2-(Benzothiazol-2-yl)-3-(3-(4-chlorophenyl)-1-phenyl-1H-pyrazol-4-yl)acrylonitrile (27). Yield: 73%, mp: 184–186 °C (dioxane). IR (cm^{-1}): 2219 (C≡N); 1642 (C=N); 1283, 1061 (C-S-C). ^{1}H-NMR (δ ppm): 7.31–7.34 (m, 3H, phenyl-$C_{3,4,5}$-H); 7.52–7.63 (m, 8H, benzothiazole-H, phenyl-$C_{2,6}$-H and *p*-chloro-$C_{2,6}$-H); 7.95 (d, *J* = 8.4 Hz, 2H, *p*-chlorophenyl-$C_{3,5}$-H); 8.22 (s, 1H, =CH); 9.26 (s, 1H, pyrazole-C_5-H). Anal. Calcd for $C_{25}H_{15}ClN_4S$ (438.93): C, 68.41; H, 3.44.; N, 12.76; S 7.31. Found: C, 68.73; H, 3.47; N, 12.95; S 7.59.

2-(Benzothiazol-2-yl)-3-(1-(4-nitrophenyl)-3-phenyl-1H-pyrazol-4-yl)acrylonitrile (28). Yield: 81%, mp: 176–178 °C (dioxane). IR (cm^{-1}): 2246 (C≡N); 1615 (C=N); 1290, 1088 (C-S-C). ^{1}H-NMR (δ ppm): 7.19–7.21 (m, 3H, phenyl-$C_{3,4,5}$-H); 7.43–7.51 (m, 4H, benzothiazole-H); 7.88 (d, *J* = 7.1 Hz, 2H, phenyl-$C_{2,6}$-H); 8.27 (d, *J* = 9.2 Hz, 2H, *p*-nitrophenyl-$C_{2,6}$-H); 8.37 (d, *J* = 9.2 Hz, 2H, *p*-nitrophenyl-$C_{3,5}$-H); 8.55 (s, 1H, =CH); 9.32 (s, 1H, pyrazole-C_5-H). Anal. Calcd for $C_{25}H_{15}N_5O_2S$ (449.48): C, 66.80; H, 3.36; N, 15.58; S 7.13. Found: C, 66.67; H, 3.49; N, 15.71; S 7.45.

N-[[1-(4-nitrophenyl)-3-*p*-tolyl-1*H*-pyrazol-4-yl] methylene]-1*H*-benzimidazole-2-amine (29) and *N*-[[3-(4-Chlorophenyl)-1-(4-nitrophenyl)-1*H*-pyrazol-4-yl] methylene]-1*H*-benzimidazole-2-amine (30)

A mixture of 2-aminobenzimidazole (0.26 g, 0.002 mole) and the appropriate pyrazole aldehyde **14, 15** (0.002 mole) in dry dioxane (10 ml) containing few drops of conc. H_2SO_4 was heated under reflux for 10 h. After cooling, the precipitated product was filtered, washed with ethanol, dried and crystallized from the proper solvent.

N-[[1-(4-Nitrophenyl)-3-p-tolyl-1H-pyrazol-4-yl]methylene]-1H-benzimidazole-2-amine (29). Yield: 62%, mp: > 300 °C (dioxane). IR (cm^{-1}): 3327 (NH); 1631 (C=N). ^{1}H-NMR (δ ppm): 2.31 (s, 1H, CH_3); 7.16–7.19 (m, 2H, benzimidazole-$C_{5,6}$-H); 7.42 (d, *J* = 7.8 Hz, 2H, *p*-tolyl-$C_{3,5}$-H); 7.63–7.67 (m, 4H, benzimidazole-$C_{4,7}$-H and *p*-tolyl-$C_{2,6}$-H); 8.31 (d, *J* = 8.4 Hz, 2H, *p*-nitrophenyl-$C_{2,6}$-H); 8.47 (d, *J* = 8.4 Hz, 2H, *p*-nitrophenyl-$C_{3,5}$-H); 9.43 (s, 1H, pyrazole-C_5-H); 9.82 (s, 1H, N=CH); 12.10 (s, 1H, D_2O exchangeable). Anal. Calcd for $C_{24}H_{18}N_6O_2$ (422.44): C, 68.24; H, 4.29; N, 19.89. Found: C, 68.59; H, 4.40; N, 20.07.

N-[[3-(4-Chlorophenyl)-1-(4-nitrophenyl)-1H-pyrazol-4-yl] methylene]-1H-benzimidazole-2-amine (30). Yield: 59%, mp: > 300 °C (dioxane/EtOH). IR (cm^{-1}): 3330 (NH); 1628 (C=N). ^{1}H-NMR (δ ppm): 7.07–7.10 (m, 2H, benzimidazole-$C_{5,6}$-H); 7.63 (d, *J* = 8.2 Hz, 2H, *p*-chlorophenyl-$C_{2,6}$-H); 7.79–8.12 (m, 4H, benzimidazole-$C_{4,7}$-H and *p*-chlorophenyl-$C_{3,5}$-H); 8.26 (d, *J* = 8.4 Hz, 2H, *p*-nitrophenyl-$C_{2,6}$-H); 8.38 (d, *J* = 8.4 Hz, 2H, *p*-nitrophenyl-$C_{3,5}$-H); 9.55 (s, 1H, pyrazole-C_5-H); 9.99 (s, 1H, N=CH); 11.22 (s, 1H, D_2O exchangeable). Anal. Calcd for $C_{23}H_{15}ClN_6O_2$ (442.86): C, 62.38; H, 3.41; N, 18.98. Found: C, 62.49; H, 3.31; N, 18.67.

N-(1-Benzofuran-2yl-ethylidene)-*N'*-phenylhydrazine (32) and *N*-(1-benzofuran-2yl-ethylidene)-*N'*-(4-nitrophenyl) hydrazine (33)

A mixture of 2-acetylbezofuran **31** (0.96 g, 0.006 mole) and substituted phenyl hydrazine (0.006 mole) in absolute ethanol (10 ml) containing few drops of glacial acetic acid was heated under reflux for 3 h. After cooling, the precipitated product was filtered, washed with ethanol, dried and crystallized from ethanol.

N-(1-Benzofuran-2 yl-ethylidene)-N'-phenylhydrazine (32). yield: 85%, mp: 86–88 °C [reported 85–87 °C] [28]. IR (cm^{-1}): 3269 (NH); 1642 (C=N); 1213, 1042 (C-O-C). ^{1}H-NMR (δ ppm): 2.31 (s, 3H, CH_3); 7.15–7.24 (m, 3H, phenyl-$C_{3,4,5}$-H); 7.27–7.36 (m, 3H, benzofuran-$C_{3,5,6}$-H); 7.39 (d, *J* = 7.2 Hz, 2H, phenyl-$C_{2,6}$-H); 7.66 (d, *J* = 8.4 Hz, 1H, benzofuran-C_4-H); 7.69 (d, *J* = 7.65 Hz, 1H, benzofuran-C_7-H); 10.28 (s, 1H, NH, D_2O exchangeable).

N-(1-Benzofuran-2yl-ethylidene)-N'-(4-nitrophenyl)hydrazine (33). yield: 89%, mp: 98–100 °C [reported 97–99 °C] [28]. IR (cm^{-1}): 3300 (NH); 1630 (C=N); 1245, 1073 (C-O-C). ^{1}H-NMR (δ ppm): 2.33 (s, 3H, CH_3); 7.22–7.33 (m, 3H, benzofuran-$C_{3,5,6}$-H); 7.36 (d, *J* = 9.2 Hz, 2H, *p*-nitrophenyl-$C_{2,6}$-H); 7.60 (d, *J* = 8.4 Hz, 1H, benzofuran-C_4-H); 7.63 (d, *J* = 7.65 Hz, 1H, benzofuran-C_7-H); 8.15 (d, *J* = 9.2 Hz, 2H, *p*-nitrophenyl-$C_{3,5}$-H); 10.39 (s, 1H, NH, D_2O exchangeable).

3-(Benzofuran-2 yl)-1-phenyl-1*H*-pyrazole-4-carbaldehyde (34) and 3-(benzofuran-2 yl)-1-(4-nitrophenyl)-1*H*-pyrazole-4-carbaldehyde (35)

To an ice-cold dimethylformamide (2.5 g, 3 ml, 0.034 mole), $POCl_3$ (1 g, 6 ml, 0.0066 mole) was added dropwise with stirring over a period of 30 min. Stirring was continued for further 1 h keeping the reaction temperature at 0 °C. Compound **32**, **33** (0.003 mole) was then added and the reaction mixture was heated at 60–70 °C with stirring for 4 h, allowed to cool and poured onto ice-water mixture. The obtained mixture was boiled and the obtained precipitate was filtered, washed with water, dried and crystallized from the proper solvent.

3-(Benzofuran-2 yl)-1-phenyl-1H-pyrazole-4-carbaldehyde (34). Yield: 79%, mp: 118–120 °C (EtOH) [reported 116–118 °C] [28]. IR (cm^{-1}): 1710 (C=O); 1622 (C=N); 1240, 1061 (C-O-C).

^{1}H-NMR (δ ppm): 7.32 (t, *J* = 7.2 Hz, phenyl-C_4-H); 7.34–7.43 ((m, 3H, benzofuran-$C_{3,5,6}$-H); 7.60 (t, *J* = 7.8 Hz, 2H, phenyl-$C_{3,5}$-H); 7.71 (d, *J* = 8.1 Hz, 1H, benzofuran-C_4-H); 7.77 (d, *J* = 7.65 Hz, 1H, benzofuran-C_7-H); 8.00 (d, *J* = 8.4 Hz, 2H, phenyl-$C_{2,6}$-H); 9.40 (s, 1H, pyrazole-C_5-H); 10.22 (s, 1H, CHO). Anal. Calcd for $C_{18}H_{12}N_2O_2$ (288.30): C, 74.99; H, 4.20; N, 9.72. Found: C, 75.06; H, 4.28; N, 9.83.

3-(Benzofuran-2 yl)-1-(4-nitrophenyl)-1H-pyrazole-4-carbaldehyde (35). Yield: 81%, mp: 126–128 °C (dioxane) [reported 125–127 °C] [28]. IR (cm^{-1}): 1712 (C=O); 1610 (C=N); 1225, 1041 (C-O-C). ^{1}H-NMR (δ ppm): 7.29–7.40 ((m, 3H, benzofuran-$C_{3,5,6}$-H); 7.67 (d, *J* = 8.1 Hz, 1H, benzofuran-C_4-H); 7.75 (d, *J* = 7.65 Hz, 1H, benzofuran-C_7-H); 8.12 (d, *J* = 9.2 Hz, 2H, p-nitrophenyl-$C_{2,6}$-H); 8.35 (d, *J* = 9.2 Hz, 2H, p-nitrophenyl-$C_{3,5}$-H); 9.38 (s, 1H, pyrazole-C_5-H); 10.31 (s, 1H, CHO). Anal. Calcd for $C_{18}H_{11}N_3O_4$ (333.30): C, 64.86; H, 3.33; N, 12.61. Found: C, 64.90; H, 3.56; N, 12.80.

General procedure for preparation of compounds (36–39)

A mixture of the appropriate aldehyde **34**, **35** (0.002 mole) and the appropriate thiosemicarbazide or acid hydrazide in ethanol (10 ml) containing few drops of glacial acetic acid was refluxed for 4 h. After cooling, the precipitated product was filtered, washed with ethanol, dried and crystallized from the proper solvent.

1-((3-Benzofuran-2-yl)-1-phenyl-1H-pyrazol-4-yl)methylene)-4-cyclohexylthiosemicarbazide (36). Yield: 83%, mp: 264–266 °C (dioxane). IR (cm^{-1}): 3296 (NH); 1632 (C=N); 1266, 1088 (C-O-C). ^{1}H-NMR (δ ppm): 1.10–1.22 (m, 4H, cyclohexyl-$C_{3,5}$-H); 1.51–1,72 (m, 6H, cyclohexyl-$C_{2,4,6}$-H); 2.53 (m, 1H, cyclohexyl-C_1-H); 7.18–7.88 (m, 10H, aromatic-H); 8.71 (s, 1H, CH=N); 9.27 (s, 1H, pyrazole-C_5-H); 9.75 and 11.48 (2 s, each 1H, 2NH, D_2O exchangeable). Anal. Calcd for $C_{25}H_{25}N_5OS$ (443.56): C, 67.69; H, 5.68; N, 15.79; S 7.23. Found: C, 67.55; H, 5.79; N, 15.55; S 7.51.

1-((3-Benzofuran-2-yl)-1-phenyl-1H-pyrazol-4-yl)methylene)-4-phenylthiosemicarbazide (37). Yield: 79%, mp: 240–242 °C (dioxane). IR (cm^{-1}): 3300 (NH); 1611 (C=N); 1258, 1047 (C-O-C). ^{1}H-NMR (δ ppm): 7.20–7.91 (m, 15H, aromatic-H); 8.74 (s, 1H, CH=N); 9.31 (s, 1H, pyrazole-C_5-H); 9.98 and 11.93 (2 s, each 1H, 2NH, D_2O exchangeable). Anal. Calcd for $C_{25}H_{19}N_5OS$ (437.52): C, 68.63; H, 4.38; N, 16.01; S 7.33. Found: C, 68.83; H, 4.37; N, 15.83; S 7.46.

N'-((3-Benzofuran-2-yl)-1-phenyl-1H-pyrazol-4-yl)methylene) benzohydrazide (38). Yield: 76%, mp: 246–248 °C (dioxane/EtOH). IR (cm^{-1}): 3250 (NH); 1660 (C=O); 1609 (C=N); 1250, 1061 (C-O-C). ^{1}H-NMR (δ ppm): 7.25–8.70 (m, 15H, aromatic-H); 8.80 (s, 1H, CH=N); 9.23 (s, 1H, pyrazole-C_5-H); 12.08 (s, 1H, NH, D_2O exchangeable). Anal. Calcd for $C_{25}H_{18}N_4O_2$ (406.44): C, 73.88; H, 4.46; N, 13.78. Found: C, 73.69; H, 4.31; N, 13.91.

N'-((3-Benzofuran-2-yl)-1-phenyl-1H-pyrazol-4-yl)methylene) isonicotinohydrazide (39). Yield: 71%, mp: 236–238 °C (EtOH). IR (cm^{-1}): 3207 (NH); 1667 (C=O); 1621 (C=N); 1236, 1069 (C-O-C). ^{1}H-NMR (δ ppm): 7.28–7.85 (m, 10H, aromatic-H); 7.89 (d, *J* = 7.4 Hz, 2H, pyridyl-$C_{2,6}$-H); 8.78 (d, *J* = 7.4 Hz, 2H, pyridyl-$C_{3,5}$-H); 8.82 (s, 1H, CH=N); 9.11 (s, 1H, pyrazole-C_5-H); 12.16 (s, 1H, NH, D_2O exchangeable). Anal. Calcd for $C_{24}H_{17}N_5O_2$ (407.42): C, 70.75; H, 4.21; N, 17.19. Found: C, 70.57; H, 4.15; N, 17.03.

3-(3-Benzofuran-2-yl)-1-aryl -1H-pyrazol-4-yl)-1-arylprop-2-en-1-one (40–42)

An equimolar mixture of the substituted pyrazolecarboxaldehyde **34, 35** (0.01 mole) and the appropriate acetophenone in ethanolic KOH (3%) (30 mL) was stirred at room temperature for 4 h. The precipitate formed was filtered, washed with EtOH, dried and crystallized from the appropriate solvent.

3-(3-Benzofuran-2-yl)-1-phenyl-1H-pyrazol-4-yl)-1-phenylprop-2-en-1-one (40). Yield: 67%, mp: 215–217 °C (dioxane/EtOH). IR (cm^{-1}): 1665 (C=O), 1620 (C=N); 1244, 1050 (C-O-C). ^{1}H-NMR (δ ppm): 7.21–7.81 (m, 17H, aromatic-H and CH=CH); 9.39 (s, 1H, pyrazole-C_5-H). Anal. Calcd for $C_{26}H_{18}N_2O_2$ (390.43): C, 79.98.; H, 4.65; N, 7.17. Found: C, 80.17; H, 4.83; N, 7.44.

3-(3-Benzofuran-2-yl)-1-phenyl-1H-pyrazol-4-yl)-1-(4-chlorophenyl)prop-2-en-1-one (41). Yield: 77%, mp: 210–212 °C (EtOH). IR (cm^{-1}): 1660 (C=O), 1625 (C=N); 1267, 1072 (C-O-C). ^{1}H-NMR (δ ppm): 7.22–7.89 (m, 16H, aromatic-H and CH=CH); 9.41 (s, 1H, pyrazole-C_5-H). MS, m/z (rel. Abund. %): 426 (6.0) M^{+}+2; 425 (6.0) M^{+}+1; 424 (13.4) M^{+}; 286 (19.8); 285 (100); 182 (7.4); 155 (7.4); 139 (29.7); 127 (8.1); 113 (10.2); 111 (27.2); 89 (9.5); 77 (56.2); 75 (18.0); 69 (9.9); 63 (10.2); 51 (26.1); 50 (10.6). Anal. Calcd for $C_{26}H_{17}ClN_2O_2$ (424.88): C, 73.50; H, 4.03; N, 6.59. Found: C, 73.19; H, 4.19; N, 6.63.

3-(3-Benzofuran-2-yl)-1-(4-nitrophenyl)-1H-pyrazol-4-yl)-1-(4-chlorophenyl)prop-2-en- 1-one (42). Yield: 81%, mp: 234–236 °C (dioxane). IR (cm^{-1}): 1662 (C=O), 1621 (C=N); 1247, 1061 (C-O-C). ^{1}H-NMR (δ ppm): ^{1}H-NMR (δ ppm): 7.25–8.07 (m, 11H, aromatic-H and CH=CH); 8.12 (d, J = 9.2 Hz, 2H, *p*-nitrophenyl-$C_{2,6}$-H); 8.39 (d, J = 9.2 Hz, 2H, *p*-nitrophenyl-$C_{3,5}$-H); 9.54 (s, 1H, pyrazole-C_5-H). Anal. Calcd for $C_{26}H_{16}ClN_3O_4$ (469.88): C, 66.46; H, 3.43; N, 8.94. Found: C, 66.75; H, 3.44; N, 8.68.

Antiangiogenesis activity[29]

In Vitro cytotoxicity assay

MCF-7 human breast cancer cell line was grown in RPMI 1640 medium containing 10% fetal bovine serum and 2 mM L-glutamine. Colo-205 human colon cancer and Hep-2G cells were grown in DMEM medium containing 10% fetal bovine serum and 2 mM L-glutamine. Human umbilical venous endothelial cells (HUVECs) were grown in M-199 supplemented with heparin (5 U·mL^{-1}) endothelial cell growth supplement (ECGS, 200 mg·mL^{-1}) and 20% FBS. Cells were inoculated into 96 well microtiter plates in 100 µl at plating densities ranging from 5000 to 40000 cells/well. After cell inoculation, the microtiter plates were incubated at 37 °C, 5% CO_2, 95% air and 100% relative humidity for 24 h. After 24 h, a plate of MCF-7 and HUVEC lines were fixed in situ with trichloroacetic acid (TCA), to represent a measurement of the cell population at the time of compounds addition. Tested compounds were solubilized in dimethyl sulfoxide at 400-fold the desired final tested concentrations. Serial dilutions were made to provide a total of different concentrations of tested compounds plus control. Aliquots of 100 µl of tested compound dilutions were added to the appropriate microtiter wells containing 100 µl of medium, resulting in the required final drug concentrations. The plates were incubated

for an additional 48 h at 37 °C, 5 % CO_2, 95 % air, and 100 % relative humidity. Cells were fixed in situ by the gentle addition of 50 µl of 50 % (w/v) 10 % TCA and incubated for 60 min at 4 °C. The supernatant was discarded, and the plates were washed 5 times with PBS and dried. Sulforhodamine B (SRB) solution (100 µl) at 0.4 % (w/v) in 1 % acetic acid was added to each well, and plates were incubated for 10 min at room temperature. After staining, unbound dye was removed by washing several times with 1 % acetic acid and the plates were air dried. Bound stain is subsequently solubilized with 10 mM trizma base, and the absorbance was read on an automated plate reader at a wavelength of 515 nm. Dose–response cure was calculated.

HUVECs growth inhibition assay [30]

HUVECs at a concentration of (2×10^3) were plated in a 96-well plate in 200 ml of M-199 medium. After 24 h, the test compound (100 µl) was added to each well at different concentrations in M-199 medium. On day 0, one plate is stained with 0.5 % crystal violet in 20 % methanol for 10 min, rinsed with PBS. The remaining plates are incubated for 72 h at 37 °C. After 72 h, plates were stained with 0.5 % crystal violet in 20 % methanol, rinsed with PBS and dried. The stain is eluted with (1:1) solution of ethanol: 0.1 M sodium citrate (including day 0 plate), and absorbance is measured at 540 nm with an ELISA reader. Day 0 absorbance is subtracted from the 72 h plates and data is plotted as percentage of control proliferation (vehicle treated cells). IC_{50} (drug concentration causing 50 % inhibition) was calculated from the plotted data.

Cord formation assay [31]

Matrigel (100 µl of 5 mg/ml) was placed in each well of an ice-cold 96-well plate. The plate is allowed to sit at room temperature for 15 min then incubated at 37 °C for 30 min to permit the matrigel to polymerize. HUVEC were prepared in M-199 medium at a concentration of (2×10^5) cells/ml. The tested compounds were prepared at different concentrations (5 concentration levels) in the same medium. Equal amounts of cells suspension and tested compounds (500 µl/each) are mixed and 200 µl of this suspension are placed in triplicate on the polymerized matrigel. After 24 h incubation, pictures were taken in triplicate for each concentration using a Bioquant Image Analysis system. Drug effect (IC_{50}) is assessed compared to untreated controls by measuring the length of cords formed and number of junctions.

Cell migration assay [31]

Migration is assessed using the 48-well Boyden chamber and 8 µm pore size collagen-coated according to Sultan et al. RPMI 1640 medium alone (control) or medium containing chemoattractant VEGF 20 ng/ml were added to the bottom chambers. HUVEC suspension (2×10^5 cells/ml) were prepared in (RPMI 1640 + 1 % BSA) with or without test compounds and added to the top chambers. After 24 h incubation at 37 °C, the membrane is rinsed in PBS, fixed and stained in Diff-Quick solutions. The filter is placed on a glass slide with the migrated cells facing down and cells on top are removed using a Kimwipe. The testing is performed in triplicates and 5 fields are counted from each well. Unstimulated control values are subtracted from stimulated control and drug treated values and data is plotted as mean migrated cell ± S.D. IC_{50} is calculated from the plotted data.

Modeling Studies

Computer-assisted simulated docking experiments were carried out under an MMFF94X force field in KDR structure (PDB ID: 2QU5) using Chemical Computing Group's Molecular Operating Environment (MOE-dock 2009) software, Montréal, Canada.

Results and Discussion

Chemistry

The synthetic strategies to obtain the target compounds are depicted in ○ **Fig. 5**, **6**. The key starting materials 1,3-diphenyl-1*H*-pyrazole-4-carbaldehyde **9** [32], 1-phenyl-3-*p*-tolyl-1*H*-pyrazole-4-carbaldehyde **10** [32], 3-(4-chlorophenyl)-1-phenyl-1*H*-pyrazole-4-carbaldehyde **11** [32], 3-(4-bromophenyl)-1-phenyl-1*H*-pyrazole-4-carbaldehyde **12** [32], 1-(4-nitrophenyl)-3-phenyl-1*H*-pyrazole-4-carbaldehyde **13** [33], 1-(4-nitrophenyl)-3-*p*-tolyl-1*H*-pyrazole-4-carbaldehyde **14**, 3-(4-chlorophenyl)-1-(4-

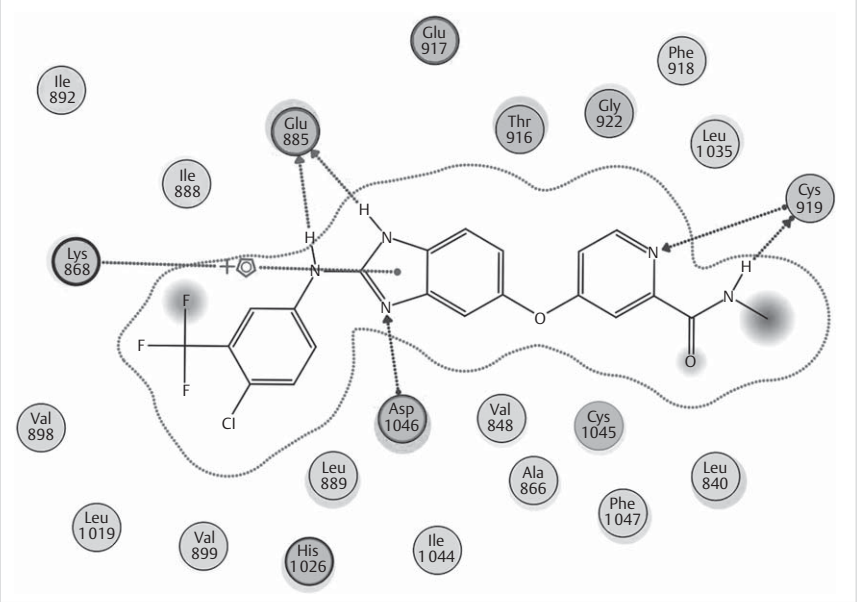

Fig. 2 Binding mode for 2-aminobenzimidazole derivative **B** docked and minimized in KDR binding pocket using MOE software.

nitrophenyl)-1*H*-pyrazole-4-carbaldehyde **15** [34], and 3-(4-bromophenyl)-1-(4-nitrophenyl)-1*H*-pyrazole-4-carbaldehyde **16** [22] were prepared from the reaction of acetophenone or 4-substituted acetophenones with phenyl hydrazine or 4-nitrophenyl hydrazine to produce the corresponding hydrazones **1–8**, followed by Vilsmeier-Haack reaction [35].

Heating the appropriate pyrazole aldehyde with the corresponding 2-(1*H*-benzimidazol-2-yl)acetonitrile or 2-(benzothiazol-2-yl)acetonitrile in absolute ethanol in the presence of triethylamine afforded the corresponding acrylonitrile **17–28**. Analogously, reaction of the pyrazole aldehyde with 2-amino-1*H*-benzoimidazole in dioxane in presence of few drops of conc.

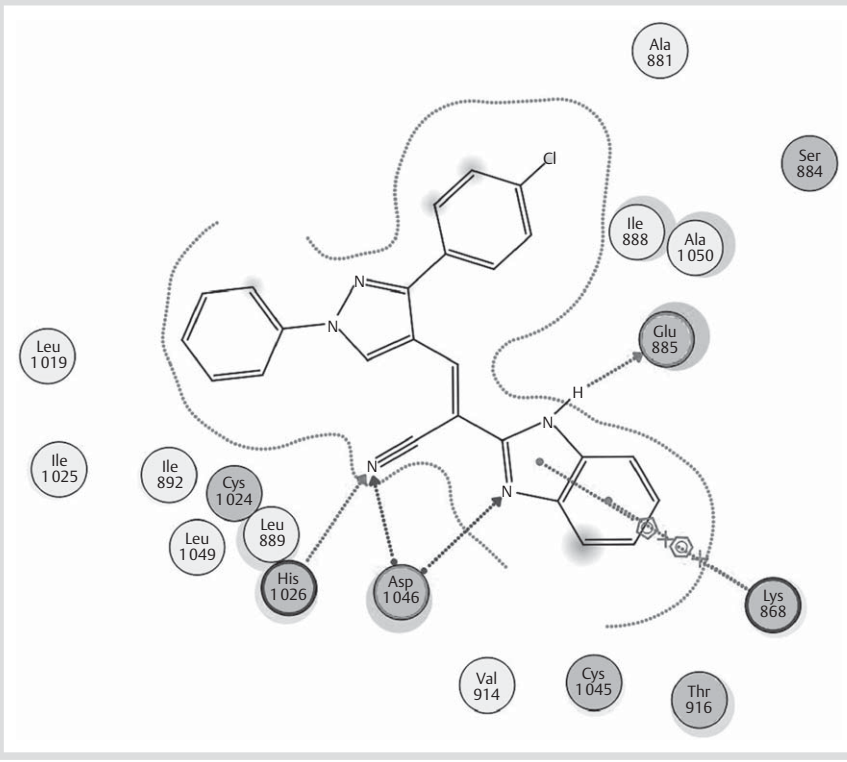

Fig. 3 Binding mode for compound **19** docked and minimized in KDR binding pocket using MOE software.

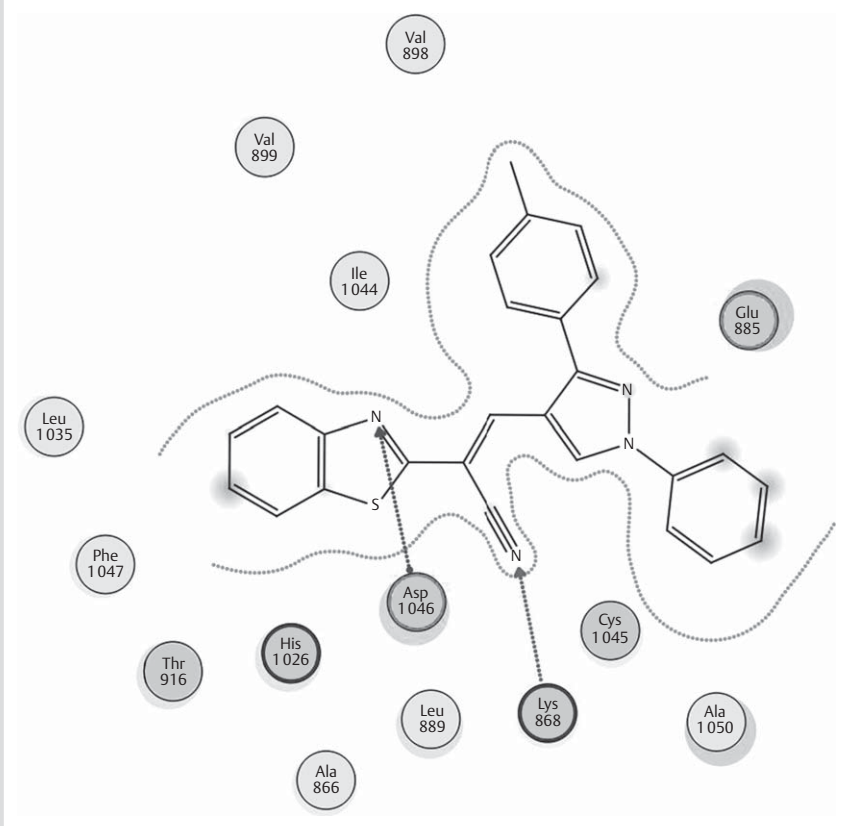

Fig. 4 Binding mode for compound **26** docked and minimized in KDR binding pocket using MOE software.

H_2SO_4 yielded the corresponding pyrazolemethylenebenzimidazol-2-amine **29, 30** (▶ **Fig. 5**).

Condensation of 2-acetylbenzofuran [36] with the appropriate phenyl hydrazine afforded the parent hydrazones **32, 33** [28]. The latter hydrazones were then treated with a mixture of phosphorousoxychloride and DMF to obtain the key intermediates; 3-(benzofuran-2-yl)-1-phenyl-1*H*-pyrazole-4-carbaldehyde **34** [28] and 3-(benzofuran-2-yl)-1-(4-nitrophenyl)-1*H*-pyrazole-4-carbaldehyde **35** [28]. These key intermediates were then reacted with the appropriate thiosemicarbazide, acid hydrazide or acetophenone to afford the corresponding thiosemicarbazone **36, 37**, hydrazone **38, 39** and chalcone derivatives **40–42**; respectively (▶ **Fig. 6**).

Antiangiogenesis activity

Angiogenesis is a complex process that includes endothelial cells proliferation, migration, alignment and formation of capillary like structures. Endothelial cells rather than tumor cells are considered as good drug candidates for diseases associated with antiangiogenesis. 12 compounds **18**, **19**, **22**, **23**, **26**, **27**, **30**, **35**, **37**, **39**, **41**, and **42** were initially evaluated for their cytotoxicity in 3 cancer cell lines tested at 10^{-4}M drug concentration (▶ **Table 1**). Cancer cell lines adopted in this prescreen were MCF-7 (Breast), Hep2G (Liver), and Colo205 (Colon). The prescreen assay aims to preliminary testing a large proportion of tested compounds and eliminating the inactive compounds. Data for each compound are reported as the percent of growth of the treated cells compared to the untreated control cells. Only compounds that reduce the growth of any one of the tested cancer cell lines to approximately 32% or less are considered active. ▶ **Table 1** revealed that all the tested compounds were cytotoxic against one or more of the tested cancer cell lines except compounds **21**, **25** and **28** which showed no cytotoxic effects.

Furthermore, compounds **19**, **23**, **26**, and **42** were selected for the antiangiogenesis testing, using HUVEC. Compounds **19**, **23**, and **26** showed no cytotoxic effects compared to compound **42** that showed a significant cytotoxic effect on the tested cancer cell lines (▶ **Table 1**).

The IC_{50} values for the tested compounds **19**, **23**, **26**, and **42** were determined as 0.29, 0.35, 0.41, and 1.82 $\mu g \cdot mL^{-1}$, respectively as described under the experimental section. Compounds **19**, **23**, **26**, and **42** were assayed at 3 different concentrations, one using IC_{50} for each tested compound as mentioned in ▶ **Table 2** and other 2 lower concentrations of 0.1, and 0.05 $\mu g \cdot mL^{-1}$ respectively. TNP-470, an established angiogenesis inhibitor, was used as a positive inhibitory control at the same above mentioned concentration as that of the tested compounds (▶ **Table 2**). Moreover, the above concentrations of the tested compounds showed complete inhibitory effects on HUVEC tube formation at their IC_{50} concentrations and at 0.1 $\mu g \cdot mL^{-1}$, indicating that 0.1 $\mu g \cdot mL^{-1}$ concentration showed no cytotoxic effect while the complete inhibition was still observed. This concentration was ranged from 2.9~18.2-fold lower than the IC_{50} value of the tested compounds against HUVECs measured under the same conditions. Besides, the comparison between IC_{50} values of the tested compounds and the 0.1 $\mu g \cdot mL^{-1}$ concentration in cancer cell lines revealed that this concentration was more than 13.5 fold lower than the average cytotoxicity (AVR-C) against the 3 tested cancer cell lines (▶ **Table 2**).

In addition, using HUVEC cells proliferation inhibition test, compounds **19**, **23**, and **26** showed an antiproliferative effect but less than that of TNP-470, positive control (▶ **Table 3**). It is interesting to point out that compounds **19**, **23**, and **26** showed no antitumor activity in the 3 tested cancer cell line, indicating that they can exert antiangiogenic activities at non-cytotoxic concentrations (▶ **Table 3**).

To mimic the final events during angiogenesis, in which HUVEC can form network of capillaries in a 3-dimensional Matrigel culture (3D), all tested compounds were examined for their ability to interfere with HUVEC function crucial to angiogenesis, the alignment of endothelial cells in a capillary-like structure. HUVEC were plated on (3D) of Matrigel culture where they aligned, forming cords, which were evident a few hours after plating. Compounds **19**, **23**, and **26** exhibited cord formation inhibitory properties but still lower than that of the positive control, TNP-470 (▶ **Table 3**).

The chemotaxis inhibition test mainly measures the ability to inhibit HUVEC cells migration in response to the specific chemoatrractant VEGF. Compounds **19**, **23**, and **26** showed significant activity with IC_{50} values within the range of 0.73~1.6 µM, and were less than TNP-470 activity under the same experimental conditions as shown in ▶ **Table 3.** Compound **19** was the most

Table 1 Growth % after incubation with 10^{-4}M of tested compounds.

Compounds	MCF-7 (Breast)	Hep2G (Liver)	Colo 205
18	29	33	19
19	89	75	71
22	22	29	36
23	83	78	90
26	94	82	98
27	19	27	36
30	25	37	39
35	20	31	44
37	26	29	32
39	22	28	38
41	28	33	41
42	15	11	18

Table 2 Cell growth inhibition in 3 different cancer cell lines.

Compounds	Cytotoxicity (IC_{50} µg mL^{-1})				
	MCF-7	Hep2G	Colo 205	AVR-C	HUVEC
19	4.9	3.6	3.25	3.9	0.29
23	3.79	2.8	2.56	3.05	0.35
26	2.39	2.68	2.44	2.5	0.41
42	1.35	1.43	1.69	1.49	1.82
Pos. con	0.4	1.2	1.0	0.86	0.21

IC_{50}: A compound's concentration produces 50% reduction in cell growth. The values were the averages from a triplicate experiment with the individual value less than 10%. AVR-C: average values of IC_{50} of 3 tested cancer cell lines

Table 3 In vitro antiangiogenesis activities of selected compounds on tested HUVECS.

Compounds	IC_{50} (µM)		
	Proliferation inhibition	Cord formation inhibition	Chemotaxis
19	5.1	8.1	0.73
23	9.3	11.0	1.1
26	10.8	11.6	1.6
42	34.6	43.0	21.3
TNP-470 (ST)	0.005	1.12	0.42

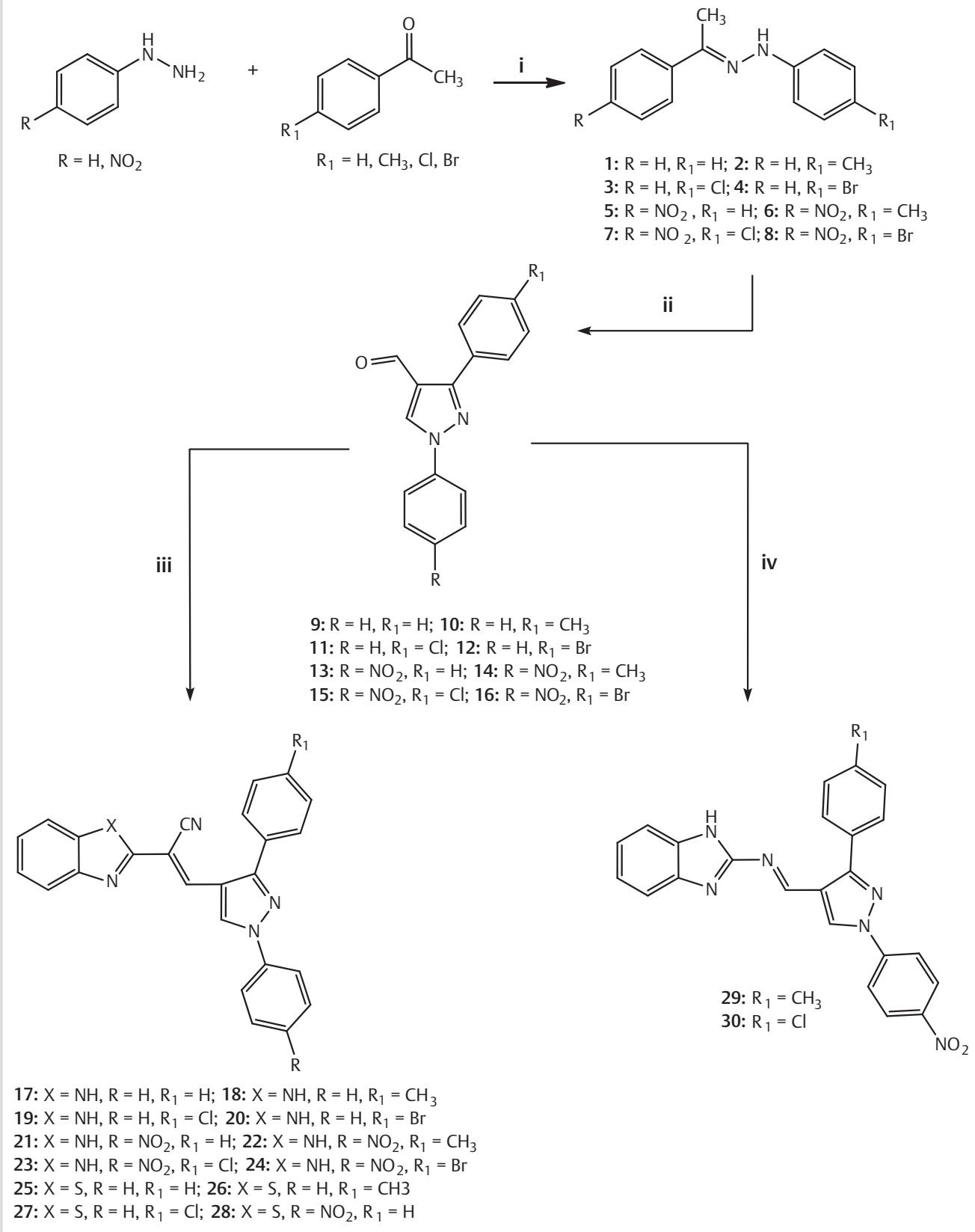

Fig. 5 Reagents and reaction conditions: **i** gl HAc, EtOH, reflux; **ii** $POCL_3$/DMF, 60–70 °C; **iii** benzazole-2-ylacetonitrile, Et_3N, EtOH, reflux, 1–3 h.; **iv** 2-aminobenzimidazole, H_2SO_4, dioxane, reflux, 10 h.

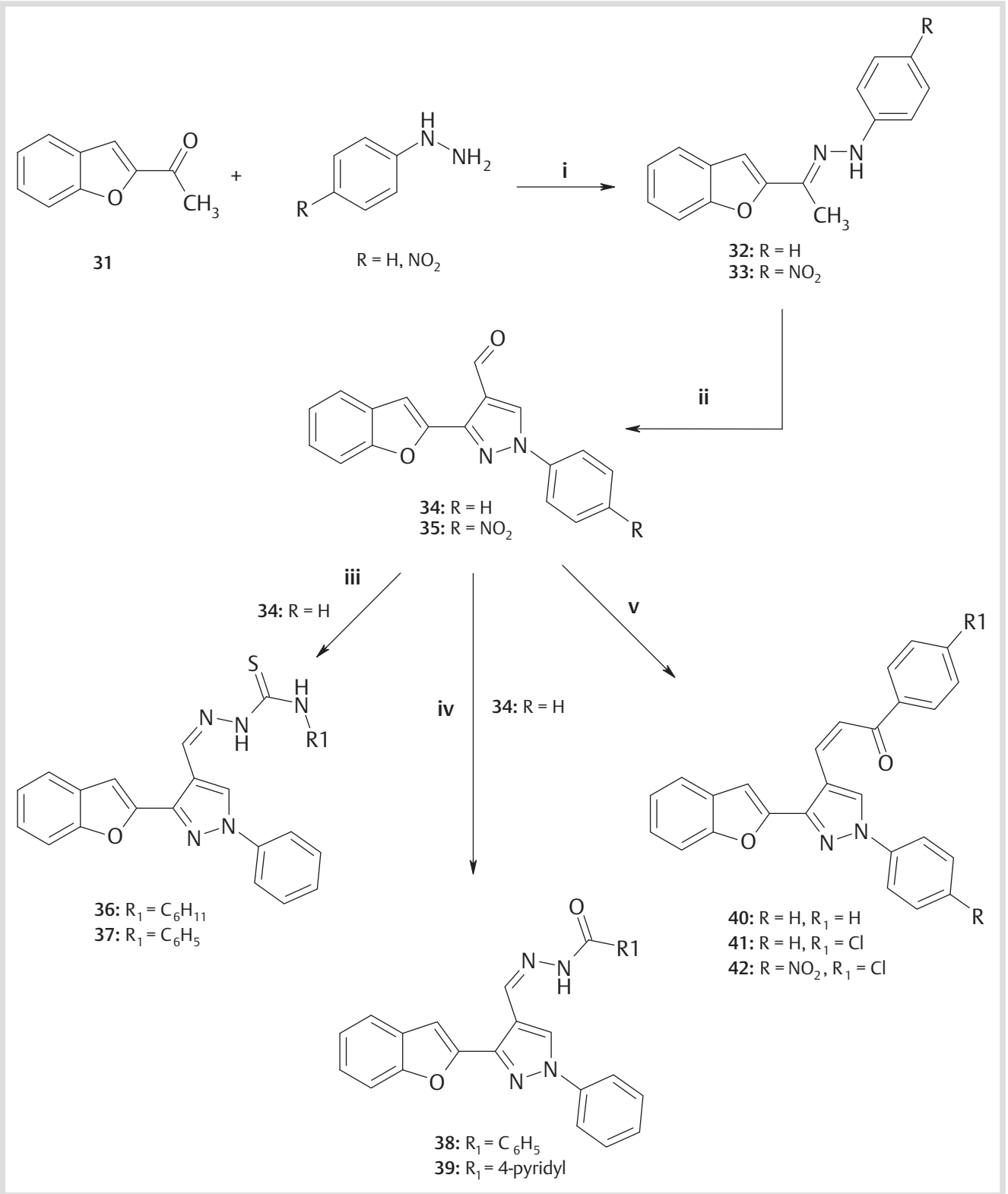

Fig. 6 Reagents and reaction conditions: **i** gl HAC, EtOH, reflux, 3 h. **ii** $POCL_3$/DMF, 60–70 °C; iii $R_1NHCSNHNH_2$, gl HAC, EtOH, reflux, 4 h.; **iv** $R_1CONHNH_2$, gl HAC, EtOH, reflux, 4 h.; **v** $R_1C_6H_4COCH_3$, KOH, EtOH, r.t.

active compared to compounds **23**, **26**, and **42** and data of chemotaxis activity of compound **19** was nearly comparable to TNP-470 (▶ **Table 3**). Structurally, the most active compound **19** has benzimidazole nucleus, unsubstituted phenyl ring at position-1 of the pyrazole moiety and phenyl ring at position-3 substituted with chloro group (electron withdrawing group of small size). Introduction of nitro group at the 4-positon of the phenyl ring (compound **23**) or replacement of the benzimidazole moiety with its bioisostere, benzthiazole nucleus and introduction of methyl group at the 4-position of the phenyl ring at position-3 of the pyrazole moiety (compound **26**) resulted in reduction of antiangiogenic activity.

It is well known that antiangiogenic activity pattern of TNP-470 is due to its effect on endothelial cells proliferation rather than motility and cord formation. In contrast, the antiangiogenic activity pattern of compounds **19**, **23** and **26** was apparently attributed to cell motility inhibition rather than proliferation, indicating that the antiangiogenic action of the above tested compounds may be mediated through different mechanisms of action from that reported to previously known compounds.

Docking Study

The docking study was carried out using the enzyme parameters obtained from the crystallographic structure of the complex between KDR with the co-crystallized 2-aminobenzimidazole derivative **B** (PDB ID: 2QU5) [23]. The docking simulation for the ligands was carried out using molecular operating environment (MOE) software supplied by the Chemical Computing Group, Inc., Montréal Canada [37].

The X-ray co-crystal structure of the complex between KDR and 2-aminobenzimidazole derivative reveals that the benzimidazole core is oriented in the hydrophobic pocket surrounded by Asp 1046 and Phe 1047 in addition, it displayed arene-arene interaction with Lys 868. The endocyclic nitrogen of the benzimidazole hydrogen bonds with the NH of Asp 1046 and either the exocyclic or the endocyclic NH may interact with the side chain of Glu 885. Hydrogen bonds are also observed between the hinge-region Cys 919 and both the nitrogen of the pyridine and the carboxamide-NH (**Fig. 2**).

Fig. 3 shows binding mode of compound **19** docked and minimized in the KDR binding pocket. In this case, hydrogen bonding is observed between NH of benzimidazole and the oxygen of Glu 885. Hydrogen bonding is also seen between the NH of Asp 1046 and both cyano group nitrogen and the endocyclic nitrogen of the benzimidazole. Cyano group nitrogen also hydrogen bonds with His 1026. In addition, benzimidazole ring of compound **19** displayed arene-arene interaction with Lys 868.

In **Fig. 4**, the benzimidazole ring of compound **26** is surrounded by hydrophobic residues Asp 1046 and Phe 1047. The endocyclic nitrogen of the benzimidazole hydrogen bonds with the NH of Asp 1046. Hydrogen bond is also observed between nitrogen cyano group and NH of Lys 868.

The docking study shows that compound **19** forms hydrogen bonds with the same residues (Glu 885 and Asp 1046) as that observed in the crystal structure of 2-aminobenzimidazole derivative with KDR. Whereas, Compound **26** having benzothiazole ring form hydrogen bond with only one residue (Asp 1046) as that observed in the X-ray co-crystal structure of the complex.

Moreover, compound **19** have a binding pattern in KDR binding site which is close to the pattern observed in the crystallographic structure of the complex between KDR with the co-crystallized 2-aminobenzimidazole derivative. This may account for increased activity recorded for compound **19**.

From the above study, it was noticed that the double bond of compounds **19** and **26** anchor the benzimidazole ring and cyano group in the right position and impart rigidity to the molecule so it can fit in the pocket correctly.

Conclusion

In the present study, new series of benzimidazoles, benzothiazoles and benzofurans incorporating pyrazole moiety were synthesized and tested for their antiangiogenic effect. Our data indicated that benzimidazole and benzothiazole derivatives linked with substituted pyrazole through a vinyl 2 carbon bridge; **19**, **23**, and **26**, represent a new class of compounds which are non-cytotoxic but have an antiangiogenic activity profile, mainly through inhibiting the motility of endothelial cells rather than its proliferation. Compound **42**, a benzofuran ring directly attached to the pyrazole moiety through a single bond, showed a cytotoxic activity against the tested 3 cancer cell lines, but its antiangiogenesis activity was less than that of compounds **19**, **23**, and **26**.

Conflict of Interest

The authors report no conflict of interest.

References

1 *Ferrara N*. Role of vascular endothelial growth factor in physiologic and pathologic angiogenesis: therapeutic implications. Semin Oncol 2002; 29 (6 Suppl 16): 10–14
2 *Fava GA*. Affective disorders and endocrine diseases. New insights from psychosomatic studies. Psychosomatics 1994; 35: 341–353
3 *Wash DA*. Angiogenesis and arthritis. Rheumatology 1999; 38: 103–112
4 *Detmar M*. The role of VEGF and thrombospondins in skin angiogenesis. J Dermatol Sci 2000; 24 (Suppl 1): S78–S84
5 *Ferrara N*, *Alitalo K*. Clinical applications of angiogenic growth factors and their inhibitors. Nat Med 1999; 5: 1359–1364
6 *Folkman J*. Role of angiogenesis in tumor growth and metastasis. Semin Oncol 2002; 29 (6 Suppl 16): 15–18
7 *Ferrara N*. Role of vascular endothelial growth factor in the regulation of angiogenesis. Kidney Int 1999; 56: 794–814
8 *O'Reilly MS*, *Holmgren L*, *Shing Y et al.* Angiostatin: a novel angiogenesis inhibitor that mediates the suppression of metastases by a Lewis lung carcinoma. Cell 1994; 79: 315–328
9 *Ishigami SI*, *Arii S*, *Furutani M et al.* Predictive value of vascular endothelial growth factor (VEGF) in metastasis and prognosis of human colorectal cancer. Br J Cancer 1998; 78: 1379–1384
10 *Folkman J*. Fighting cancer by attacking its blood supply. Scientific American 1996; 275: 150–153
11 *Kerbel RS*. Clinical trials of antiangiogenic drugs: opportunities, problems, and assessment of initial results. J Clin Oncol 2001; 19: 45s–51s
12 *Yoshida A*, *Anand-Apte B*, *Zetter BR*. Differential endothelial migration and proliferation to basic fibroblast growth factor and vascular endothelial growth factor. Growth Factors 1996; 13: 57–64
13 *Lang Z*, *Guerrera M*, *Li R et al.* Ganglioside GD1a enhances VEGF-induced endothelial cell proliferation and migration. Biochem Biophys Commun 2001; 282: 1031–1037
14 *Veikkola T*, *Karkkainen M*, *Claesson-Welsh L et al.* Regulation of angiogenesis via vascular endothelial growth factor receptors. Cancer Res 2000; 60: 203–212
15 *Shinkaruk S*, *Bayle M*, *Lain G et al.* Vascular endothelial cell growth factor (VEGF), an emerging target for cancer chemotherapy. Curr Med Chem Anti-Cancer Agents 2003; 3: 95–117
16 *Harris PA*, *Boloor A*, *Cheung M et al.* Discovery of 5-[[4-[(2,3-dimethyl-2H-indazol-6-yl)methylamino]-2-pyrimidinyl]amino]-2-methyl-benzenesulfonamide (Pazopanib), a novel and potent vascular endothelial growth factor receptor inhibitor. J Med Chem 2008; 51: 4632–4640
17 *Loges S*, *Mazzone M*, *Hohensinner P et al.* Silencing or Fueling Metastasis with VEGF Inhibitors: Antiangiogenesis Revisited. Cancer Cell 2009; 15: 167–170
18 *Douglas NC*, *Tang H*, *Gomez R et al.* Vascular endothelial growth factor receptor 2 (VEGFR-2) functions to promote uterine decidual angiogenesis during early pregnancy in the mouse. Endocrinology 2009; 150: 3845–3854

19 *Kang KB*, *Zhu C*, *Yong SK et al.* Enhanced sensitivity of celecoxib in human glioblastoma cells: Induction of DNA damage leading to p53-dependent G1 cell cycle arrest and autophagy. Mol Cancer 2009; 8: 66–81
20 *Davies NM*, *Gudde TW*, *AWC de Leeuw M.* Celecoxib: a new option in the treatment of arthropathies and familial adenomatous polyposis. Expert opin Pharmacother 2001; 2: 139–152
21 *Swamy MV*, *Herzog CR*, *Rao CV.* Inhibition of COX-2 in colon cancer cell lines by celecoxib increases the nuclear localization of active p53. Cancer Res 2003; 63: 5239–5242
22 *Abadi AH*, *Eissa AAH*, *Hassan GS.* Synthesis of novel 1,3,4-trisubstitutes pyrazole derivatives and their evaluation as antitumor and antiangiogenic agents. Chem Pharm Bull 2003; 51: 838–844
23 *Potashman MH*, *Bready J*, *Coxon A et al.* Design, synthesis, and evaluation of orally active benzimidazoles and benzoxazoles as vascular endothelial frowth factor-2 receptor tyrosine kinase inhibitors. J Med Chem 2007; 50: 4351–4373
24 *Hasegawa M*, *Nishigaki N*, *Washio Y et al.* Discovery of novel benzimidazoles as potent inhibitors of TIE-2 and VEGFR-2 tyrosine kinase receptors. J Med Chem 2007; 50: 4453–4470
25 *Hori A*, *Imaeda Y*, *Kubo K et al.* Novel benzimidazole derivatives selectively inhibit endothelial cell growth and supress angiogenesis in vitro and in vivo. Cancer Lett 2002; 183: 53–60
26 *Amino N*, *Ideyama Y*, *Yamano M et al.* YM-201627: An orally active antitumor agent with selective inhibition of vascular endothelial cell proliferation. Cancer Lett 2006; 238: 119–127
27 *Chen P.* p-Nitrobenzohydrazide as a reagent for the identification of aldehydes and ketones. J Chin Chem Soc 1935; 3: 251–255
28 *Mahadevan KM*, *Kumar DB*, *Prakash GK et al.* Synthesis and antimicrobial investigation of some novel phenylpyrazole, azetidinone and diazenyl ethanone derivatives of benzofurans. Indian J Chem B 2007; 46B: 336–343
29 *Belotti D*, *Vergani V*, *Drudis T et al.* The microtubule-affecting drug paclitaxel has antiangiogenic activity. Clin Cancer Res 1996; 2: 1843–1849
30 *Tarabolleti G*, *Micheletti G*, *Rieppi M et al.* Antiangiogenic and antitumor activity of IDN 5390, a new taxane derivative. Clin Cancer Res 2002; 8: 1182–1188
31 *Sultan AS*, *Xie J*, *LeBaron MJ et al.* Stat5 promotes homotypic adhesion and inhibits invasive characteristics of human breast cancer cells. Oncogene 2005; 24: 746–760
32 *Bernard M*, *Hulley E*, *Molenda H et al.* Azoles. 17. Beta-(4-pyrazol) acrylic and propionic acids and their anti-inflammatory activity. Pharmazie 1986; 41: 560–562
33 *Rathelot P*, *Azas N*, *El-Kashef H et al.* 1,3-Diphenylpyrazoles: synthesis and antiparasitic activities of azomethine derivatives. Eur J Med Chem 2002; 37: 671–679
34 *Rida SM*, *Saudi MNS*, *Youssef AM et al.* Synthesis and biological evaluation of the pyrazole class of cyclooxygenase-2-inhibitors. Lett Org Chem 2009; 6: 282–288
35 *Kira MA*, *Abdel-Rahman MO*, *Gadalla KZ.* The Vilsmeier reaction-III, cyclization of hydrazones to pyrazoles. Tetrahedron Lett 1969; 10: 109–110
36 *Elliott ED.* The preparation and properties of 2-vinylbenzofuran. J Am Chem Soc 1951; 73: 754
37 Molecular Operating Environment (MOE) 2009.10, Chemical Computing Group Inc., 1010 Sherbrooke Street West, Suite 910, Montréal, H3A 2R7, Canada <http://www.chemcomp.com/>